INTERFEROMETRIC SURFACE-WAVE ACOUSTO-OPTIC TIME-INTEGRATING CORRELATORS

Norman J. Berg, Irwin J. Abramovitz, and Michael W. Casseday
U.S. Army Electronics Research and Development Command
Harry Diamond Laboratories, 2800 Powder Mill Road
Adelphi, Maryland 20783

ABSTRACT

A novel structure for a coherent-interferometric acousto-optic (AO) time-integrating correlator has been implemented by using a single surface acoustic wave (SAW) device with tilted transducers to reduce intermodulation terms. The SAW device was fabricated on Y-Z $LiNbO_3$ with a center frequency of 175 MHz, a bandwidth of 60 MHz, and a time aperture of about 10 μs. The instantaneous bandwidth of the AO correlator is determined by the spacing density of the photodetector array, with a potential of 120 MHz. Typical integration times are 30 to 40 ms, providing processing gains in excess of 10^6. Such a device is very useful in providing fast synchronization of communication links. In addition, the device can demodulate to base band and simultaneously act as a synchronization lock monitor for moderate data rates. Where processing may be limited by doppler shifts, a two-dimensional architecture has been implemented to allow full processing gain.

INTRODUCTION

Current digital and microwave technology has made possible wideband communications for space applications. These systems present unique problems for which acousto-optics (AO) may provide solutions. The relative ease in applying multiple transducers to surface acoustic wave (SAW) delay lines allows novel architectures for such signal processing functions as correlation or convolution. Where large processing gain is required, integration in time rather than space permits time-bandwidth products in excess of 10^6. Coherent, interferometric schemes provide both time (e.g., time-difference-of-arrival) and frequency information simultaneously. Two one-dimensional, SAW AO time-integrating correlators and a two-dimensional correlator incorporating these features have been constructed, and the results are presented.

ONE-DIMENSIONAL CORRELATOR ANALYSIS AND APPLICATIONS

Two-input-beam time-integrating correlator

Figure 1 illustrates the operation of a two-beam SAW AO correlator.[1] A transducer is deposited on each end of the delay line (y-cut, z-propagating lithium niobate) at an angle with respect to the perpendicular to the z-axis of Θ_{Bn}, the Bragg angle in the delay line material[2] at the correlator design center frequency, ω_0. The relative tilt between the two transducers is $2\Theta_{Bn}$. The correlator input signals, A(t) cos $\omega_A t$ and B(t) cos $\omega_B t$, generate counter-propagating SAW's which interact with two sheet beams of laser light generated from a single laser and projected into the top side of the delay line with an angle of $4\Theta_B$ between them. Here, Θ_B is the Bragg angle in air for the frequency ω_0.[2] Due to the strong angular dependence of the AO Bragg interation, the right sheet beam interacts primarily with the SAW launched by the right transducer; likewise, the left sheet beam interacts primarily with the SAW generated by the left transducer. Cross terms are down by 40 dB.[3] The diffracted light is imaged onto an integrating, square-law photodiode array. For equal sheet beams of uniform intensity the diffracted light may be described by

$$L_1(t,z) = A(t - \tfrac{z}{\upsilon}) \cos[\omega_\ell(t - \tfrac{z \sin 2\Theta_B}{c}) - \omega_A(t - \tfrac{z}{\upsilon})] \quad (1)$$

and

$$L_2(t,z) = B(t + \tfrac{z}{\upsilon}) \cos[\omega_\ell(t + \tfrac{z \sin 2\Theta_B}{c}) - \omega_B(t + \tfrac{z}{\upsilon})]. \quad (2)$$

Here, ω_ℓ is the light frequency, t is time, z is the distance along the delay line and along the photodiode array (center is z = 0), υ is the acoustic propagation velocity, and c is the free-space light velocity. The photodiode array output current is proportional to the square of the sum of $L_1(t,z)$ and $L_2(t,z)$. The significant term, the cross-product proportional to $L_1(t,z) \cdot L_2(t,z)$, may be manipulated trigonometrically to generate frequency sum and difference terms. Upon time integration, only the difference term remains, yielding an output voltage proportional to

$$V(t,z) = \int_T A(t - \tfrac{z}{\upsilon})\, B(t + \tfrac{z}{\upsilon}) \cos[\frac{2\omega_\ell z \sin 2\Theta_B}{c} + (\omega_A - \omega_B)t - (\omega_A + \omega_B)\tfrac{z}{\upsilon}]dt \quad . \quad (3)$$

Since $\sin 2\Theta_B = (\omega_0/\upsilon) / (\omega_\ell/c)$, and for $\omega_A = \omega_B$ this output voltage becomes:

$$V(t,z) = \cos[\frac{2z}{\upsilon}(\omega_0 - \omega_A)] \int_T A(t - \frac{z}{\upsilon})\, B(t + \frac{z}{\upsilon})dt. \quad (4)$$

Thus, the output voltage provides the correlation of the input signals (modulation and carrier) about the correlator design center frequency. Figure 2 shows the autocorrelation of a bi-phase signal with 2.5 MHz bandwidth at 1 MHz above ω_0. The bias level, produced by the square terms proportional to the integral of $L_1(t,z)^2 + L_2(t,z)^2$, depicts the Gaussian intensity profile of the sheet beams. This bias level may be easily removed by high pass filtering or by a subtraction of one output from a subsequent output produced with one input phase-inverted. The position of the fringe pattern is due to the relative time delay between the signals. Instantaneous bandwidths of 60 MHz at 175 MHz have been achieved with integration times of 30 to 40 ms for time apertures of 10 μs.

Single-input-beam time-integrating correlator

Since the angle of the incoming beam with respect to the SAW wavefront (transducer tilt) equals that for the diffracted beam, an inverse architecture using one input laser beam is possible, as shown in Figure 3. The output voltage from the photodiode array can be shown to be identical to that for the two-beam correlator as described by equation (4). Although intermodulation terms (the interaction of the SAW from the left transducer appearing at the right output diffracted beam and vice-versa) are suppressed by less than the 40 dB achieved with the two-beam architecture, suppression is sufficient for most applications.

The large processing gains, linearity, and time delay capabilities of the SAW time-integrating correlators make them useful as advanced signal processors. These correlators may be employed merely to provide synchronization in a communications system as a discrete version of the "sliding correlator"[4] or may be used to demodulate the signal as well as to continually monitor synchronization. Figure 4 shows the output of the correlator, with bias subtracted, for inputs consisting of an information modulated, hybrid bi-phase wideband signal and an unmodulated (information free) reference signal. The overall bandwidth was 16 MHz with a bi-phase rate of 1.3 million bits per second. Integration was sychronized with the information rate. Input signal-to-noise ratio was -30 dB.

Two-Dimensional Correlator

A two-dimensional, four product correlator has been demonstrated which features the interference between two doubly diffracted beams from perpendicular SAW delay lines. As shown in Figure 5, the initial source of the sheet beams is a single laser. Since the SAW devices are perpendicular, interaction in only one device is between light polarized perpendicular to the direction of travel of the SAW's in that device. This is the preferred polarization; for light polarized parallel to the direction of SAW propagation, the diffraction efficiency may be somewhat reduced and a broadening of the Bragg angle dependence is experienced.

The double diffraction effect[5] is diagrammed in Figure 6 for the horizontal SAW device. The light from the first diffraction is of the form:

$$L_{H_1}(t,z) = A(t - \tfrac{z}{v}) \cos[\omega_\ell(t + \frac{z \sin \Phi_1}{c}) + \omega_A (t - \tfrac{z}{v})]. \quad (5)$$

The doubly diffracted light is then of the form:

$$L_{H_2}(t,z) = A(t - \tfrac{z}{v})\, B(t + \tfrac{z}{v}) \cos[\omega_\ell(t + \frac{z \sin \Phi_1}{c}) + \omega_A (t - \tfrac{z}{v}) + \omega_B(t + \tfrac{z}{v})]. \quad (6)$$

Since $\Phi_1 = 2(\Theta_{B_1} - \Theta_{B_2})$, then $\sin \Phi_1 \approx (\omega_1/v)/(\omega_\ell/c) - (\omega_2/v)/(\omega_\ell/c)$, and equation (6) reduces to:

$$L_{H_2}(t,z) = A(t - \tfrac{z}{v})\, B(t + \tfrac{z}{v}) \cos[(\omega_\ell + \omega_A + \omega_B)\, t + \tfrac{z}{v} \Delta_H], \quad (7)$$

where $\Delta_H = (\{\omega_1 - \omega_2\} - \{\omega_A - \omega_B\})$. Here, ω_1 and ω_2 are design center frequencies for which the Bragg angles are Θ_{B_1} and Θ_{B_2}, respectively. ω_1 and ω_2 are selected to be different so that the doubly diffracted light may be separated from the undiffracted beam. Similarly, for the vertical device, the doubly diffracted light is

$$L_{V_2}(t,y) = C(t - \tfrac{y}{v})\, D(t + \tfrac{y}{v}) \cos[(\omega_\ell + \omega_C + \omega_D)\, t + \tfrac{y}{v} \Delta_V], \quad (8)$$

where $\Delta_{V_2} = (\{\omega_3 - \omega_4\} - \{\omega_C - \omega_D\})$. Those doubly diffracted beams are imaged onto a photodiode area array or a vidicon that integrates the output current which is proportional to the square of the sum of these beams. The frequency difference term derived from the cross product, which is proportional to $L_{H_2}(t,z) \cdot L_{V_2}(t,y)$, produces an output voltage

$$V(t,z,y) = \int_T A(t - \tfrac{z}{\upsilon})\ B(t + \tfrac{z}{\upsilon})\ C(t - \tfrac{y}{\upsilon})\ D(t + \tfrac{y}{\upsilon})$$

$$\cos[(\omega_A + \omega_B - \omega_C - \omega_D)t + \tfrac{z}{\upsilon}\Delta_H - \tfrac{y}{\upsilon}\Delta_V)dt. \tag{9}$$

If $(\omega_A + \omega_B) = (\omega_C + \omega_D)$, then equation (9) reduces to

$$V(t,z,y) = \cos[\tfrac{z}{\upsilon}\Delta_H - \tfrac{y}{\upsilon}\Delta_V] \int_T A(t - \tfrac{z}{\upsilon})$$

$$B(t + \tfrac{z}{\upsilon})\ C(t - \tfrac{y}{\upsilon})\ D(t - \tfrac{y}{\upsilon})\ dt. \tag{10}$$

For $(\omega_1 - \omega_2) = (\omega_A - \omega_B)$ and $(\omega_3 - \omega_4) = (\omega_C - \omega_D)$, this further reduces to:

$$\int_T A(t - \tfrac{z}{\upsilon})\ B(t + \tfrac{z}{\upsilon})\ C(t - \tfrac{y}{\upsilon})$$

$$D(t + \tfrac{y}{\upsilon})dt. \tag{11}$$

Thus, this device provides a two-dimensional, four-product correlation. It has the additional ability to measure some degree of deviation from design frequencies. The usefulness of this correlator for processing signals containing doppler shifts in frequency can be shown by replacing the generalized input signals to the vertical SAW delay line, $C(t) \cos \omega_C t$ and $D(t) \cos \omega_D t$, by linear FM chirps, $\cos (\omega_C + \alpha t)t$ and $\cos (\omega_D - \alpha t)t$. Equation (8) becomes:

$$L_{V_2}(t,y) = \cos[(\omega_\ell + \omega_C + \omega_D)t + \tfrac{y}{\upsilon}\Delta_H$$

$$- 4\alpha\,(\tfrac{y}{\upsilon})t]. \tag{12}$$

The output voltage then becomes

$$V(t,z,y) = \int_T A(t - \tfrac{z}{\upsilon})\ B(t + \tfrac{z}{\upsilon})\ \cos[\omega_A +$$

$$\omega_B - \omega_C - \omega_D)t + \tfrac{z}{\upsilon}\Delta_H - \tag{13}$$

$$\tfrac{y}{\upsilon}\Delta_V + 4\alpha(\tfrac{y}{\upsilon})t]dt.$$

If $\omega_B = \omega'_B + \omega_{DP}$ where ω_{DP} is an unknown doppler shift and $\omega_A + \omega'_B = \omega_C + \omega_D$, then equation (13) reduces to

$$V(t,z,y) = \int_T A(t - \tfrac{z}{U})\, B(t + \tfrac{z}{U})$$

$$\cos[(\omega_{DP} + 4\alpha \tfrac{V}{U})t + \tfrac{z}{U}\,\Delta_H - \tfrac{y}{U}\,\Delta_V]dt. \qquad (14)$$

It can be seen that there is a y position for which $\omega_{DP} = -4\alpha \frac{y}{U}$ and the doppler shift is compensated. As an ambiguity function processor, correlation of a bi-phase code in the horizontal dimension provides range information, and doppler compensation in the vertical dimension provides velocity data. A four-product correlator has been implemented, and the output is shown in figure 7, where $_H$ and $_V$ are nonzero. The correlation spot has been moved from the center of the vidicon output by time delay (simulated range) and carrier frequency shift (simulated doppler). Bias subtraction has been performed using a video image processor.

SUMMARY

One- and two-dimensional interferometric time-integrating, acousto-optic correlators have been demonstrated. These offer large processing gains for application to wideband signal processing systems. Potential uses for synchronization, demodulation, and ambiguity function processing have been discussed.

References

1. N.J. Berg, I.J. Abramovitz, J.N. Lee, and M.W. Casseday, "A New Surface Wave Acousto-Optic Time Integrating Correlator," Appl. Phys. Lett., 36(4), pp. 256-258, 1980.

2. R. Adler, "Interaction Between Light and Sound," IEEE Spectrum 4, pp. 42-54, May 1967.

3. J.N. Lee, N.J. Berg, and M.W. Casseday, "Multichannel Signal Processing Using Acousto-optic Techniques," IEEE J. Quant. Electron ., QE-15 (11), pp. 1210-1215, Nov. 1979.

4. N.J. Berg, M.W. Casseday, I.J. Abramovitz, and J.N. Lee, "Radar and Communications Band Signal Processing Using Time-Integration Processors," SPIE, 232, Proc. 1980 IOCC, pp. 101-107, 1980.

5. J.N. Lee, N.J. Berg, and M.W. Casseday, "Multichannel Surface Acoustic Wave Correlation and Convolution with Acousto-Optic Processors," Proc. 1979 Ultrasonic Symposium, pp.34-39, 1979.

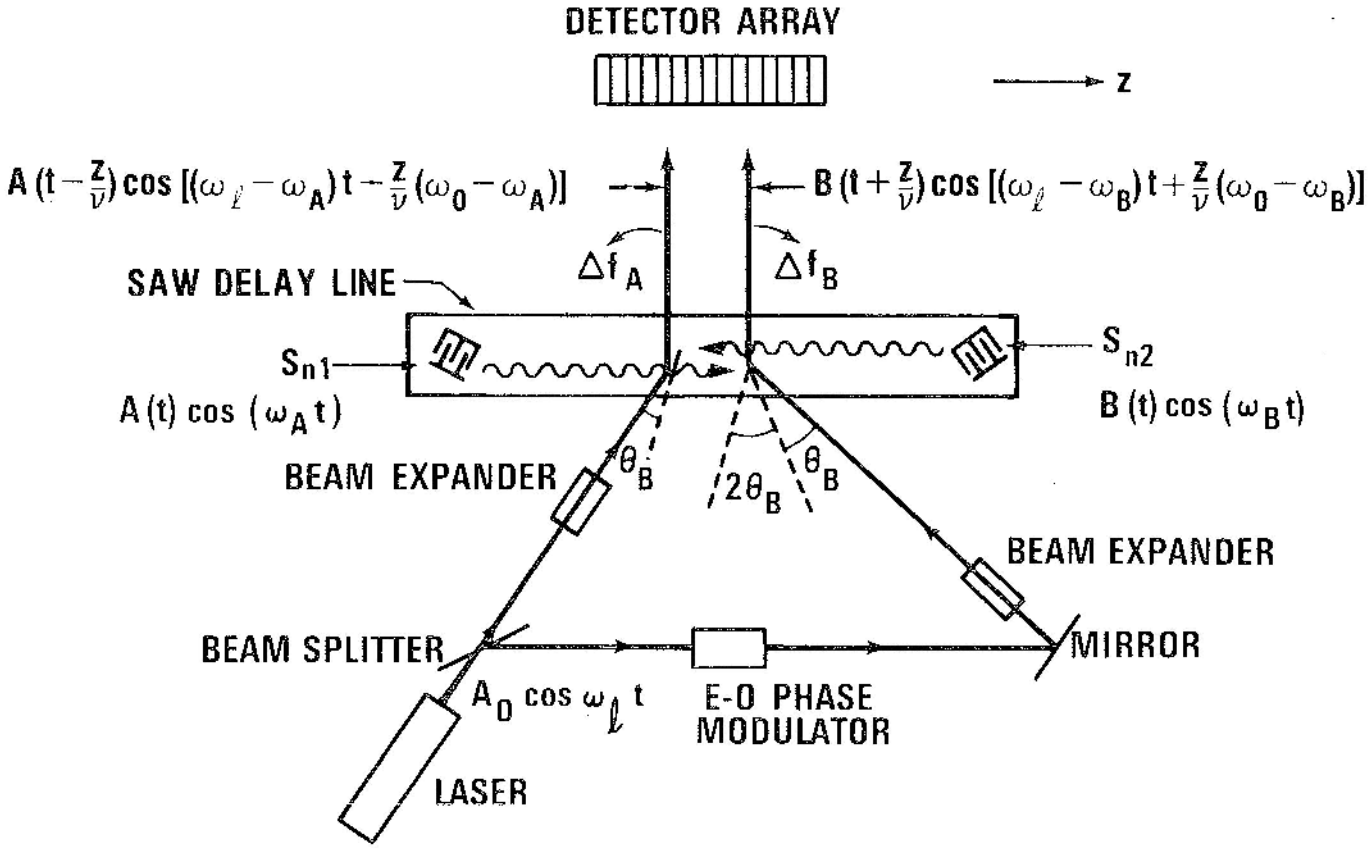

Figure 1.-Two-beam SAW time-integrating correlator.

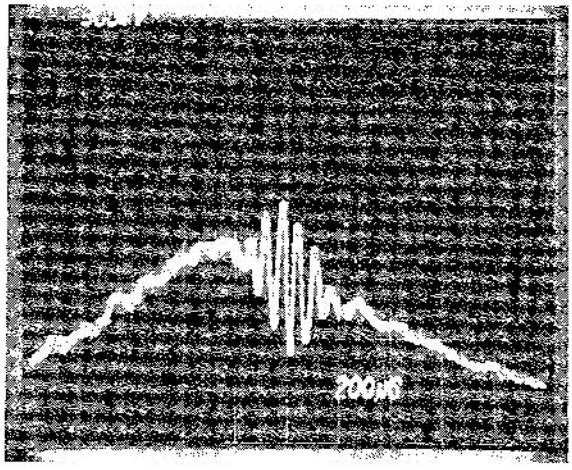

Figure 2.-Correlator output for direct sequence code at ω_0 = 1 Mhz.

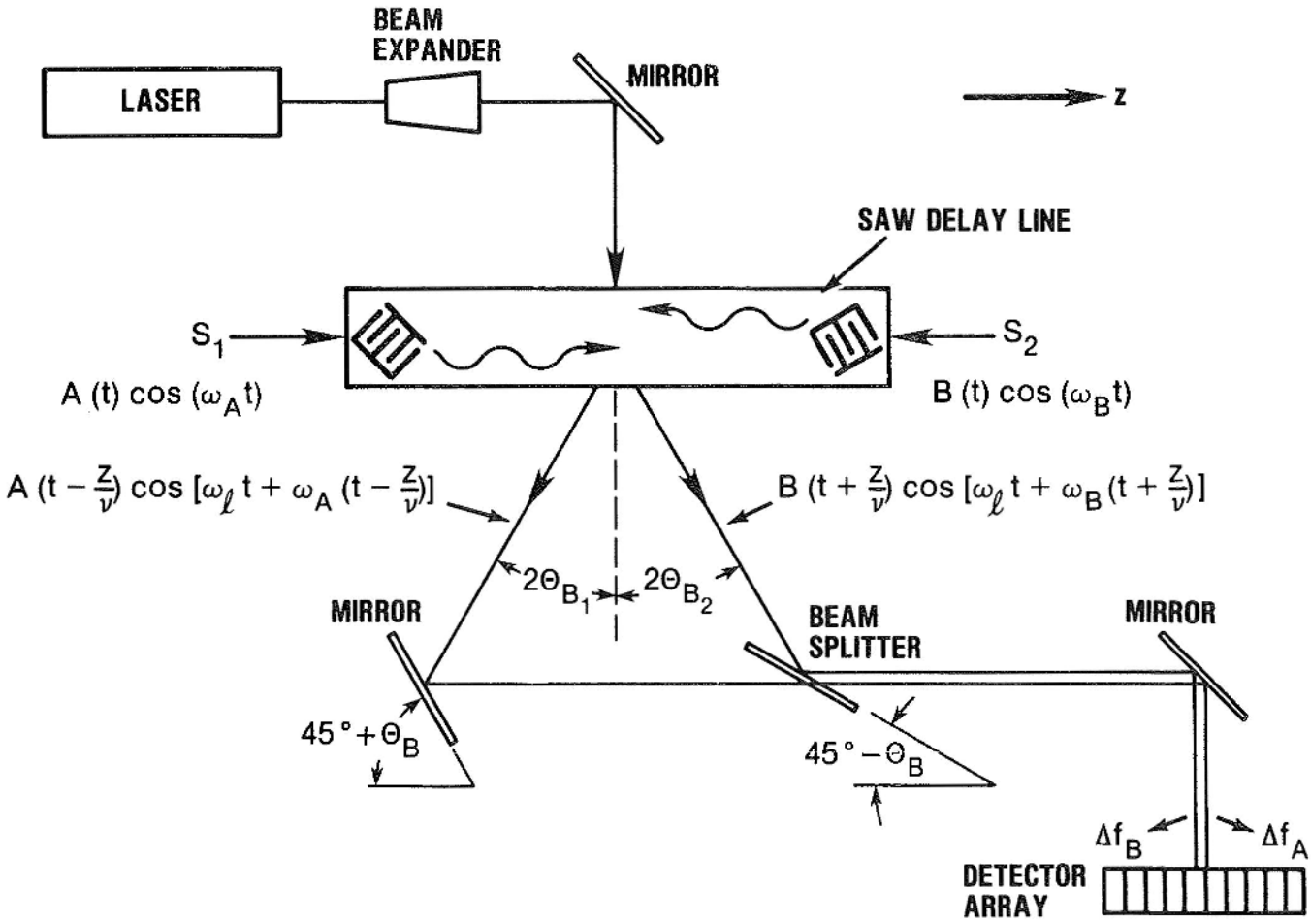

Figure 3.-Single input beam SAW AO time-integrating correlator.

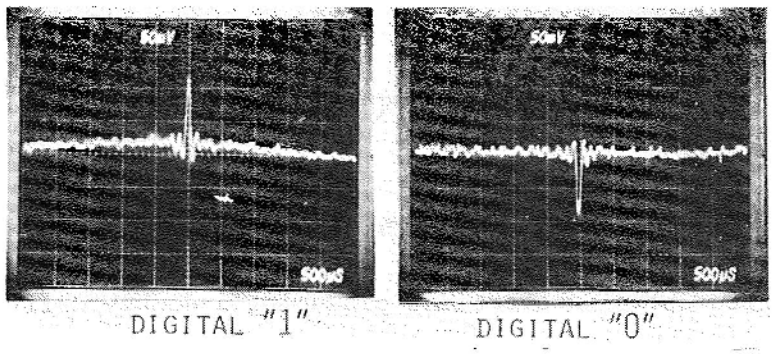

Figure 4.- Output of correlator for hybrid bi-phase signals showing demodulation.

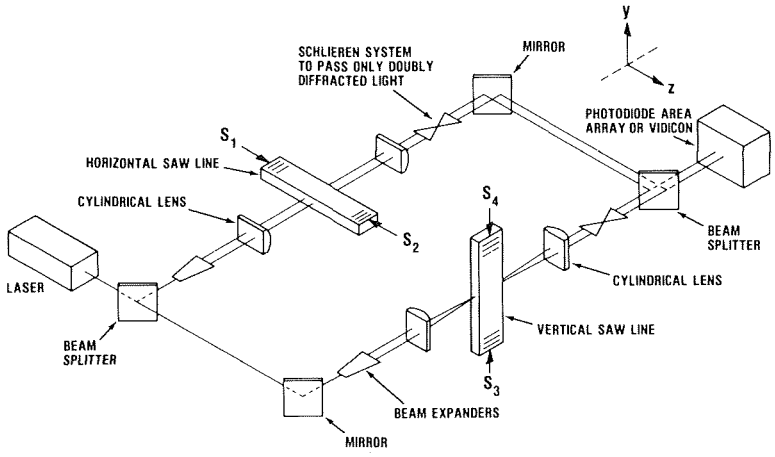

Figure 5.-Two-dimensional SAW AO time-integrating correlator.

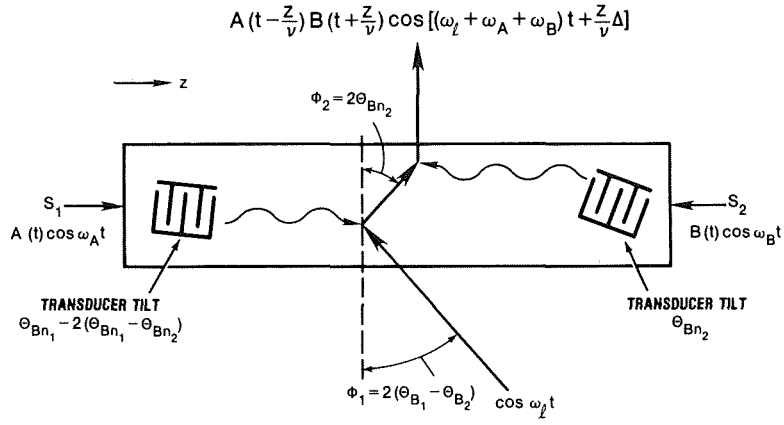

Figure 6.-Acousto-optic interactions producing a doubly diffracted beam.

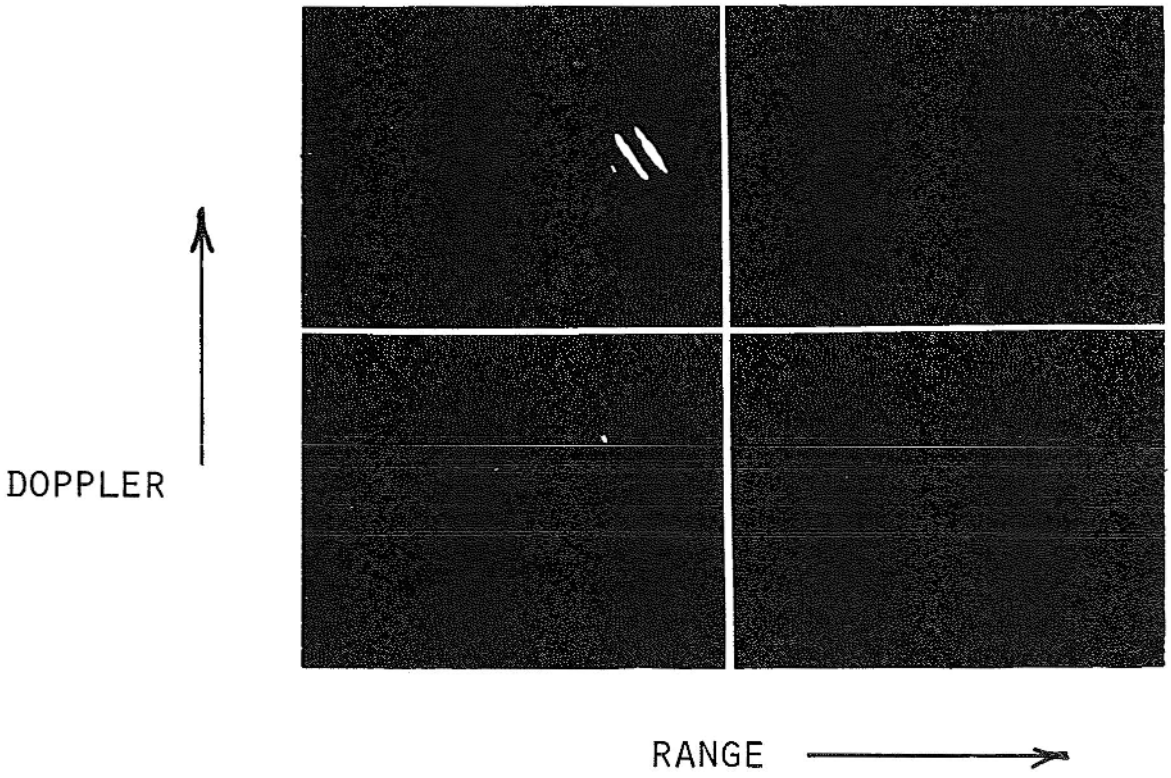

Figure 7.-Output of the four product correlator after bias subtraction.